Received 23 February 2024; revised 28 March 2024; accepted 28 March 2024. Date of publication 10 April 2024; date of current version 27 May 2024.

Digital Object Identifier 10.1109/OJAP.2024.3384397

RF-MEMS Switch for Reconfigurable With Half-Moon Slots on Elliptical-Shaped Patch Antenna for 5G Applications

KETAVATH KUMAR NAIK (Senior Member, IEEE), AND BOKKISAM VENKATA SAI SAILAJA

Department of Electronics and Communication Engineering, Koneru Lakshmaiah Education Foundation Deemed to be University, Guntur 522502, India

CORRESPONDING AUTHOR: K. K. NAIK (e-mail: drkumarkn@hotmail.com)

This work was supported in part by the SERB, Department of Science and Technology, New Delhi, India, under Grant SB/FTP/ETA-0179/2014 and Grant EEQ/2016/000754, and in part by the CSIR-SRF, Government of India under the File under Grant 09/1068(0004)2020-EMR-1.

ABSTRACT A compact dual-band reconfigurable elliptical-shaped patch antenna designed in this article. The proposed patch antenna with rectangular strip lines and an elliptical with half-moon slots presented to operate dual bands. To achieve the reconfigurability, RF-MEMS switches proposed on rectangular strip lines of the patch antenna. The capacitive shunt type RF-switch designed the proposed elliptical antenna to operate at 5G applications. The displacement of the proposed RF-MEMS switch with an air gap of 3μm, the actuation of 5.02 V, and the stress of the proposed beam is bearable up to 85.7 MPa is observed. The reconfigurable elliptical-shaped patch antenna resonates at 8.34 GHz and 10.47 GHz with a reflection coefficient of −32.28 dB and −22.7 dB respectively. The operating frequencies and gains are observed at the RF-MEMS switch placed on a patch for dual bands for four states. At the state-I, two operating frequencies and gain are 8.4G Hz, and 10.52G Hz with 2.28 dBi, and 2.18 dBi. Similarly, state-II frequencies are 8.56 GHz, and 10.55 GHz with gains of 2.08 dBi, and 1.30 dBi; state-III frequencies are 8.49 GHz, 10.47 GHz with gains of 2.48 dBi, and 3.04 dBi; and state-IV, frequencies are 8.49 GHz, 10.49 GHz with gain of 2.58 dBi, and 2.64 dBi. The compact elliptical patch antenna was simulated and a measured value is presented in this article and also both values are agreed.

INDEX TERMS 5G applications, elliptical antenna, half-moon slots, reconfigurable antenna, RF-switch.

I. INTRODUCTION

NOWADAYS communication systems require minimal-size prototype model wireless devices, and effective microwave circuits to be used for multiband applications [1], [2]. Because of their tremendous features, for example, multi-band functionality, the size, and cost of an antenna while enhancing the implementation of an RF system, reconfigurable antennas have been exclusively considered nowadays [3], [4]. Such antennas can encourage different solutions in a minimized structure and those can be used in future wireless communication applications [1]. Dynamic components, for example, switches or capacitors facilitate the antenna system to change its polarization, frequency, and radiation patterns by utilizing various approaches [2], [5]. A hex decagonal patch antenna is presented [6] and resonates with dual operating bands having high gain with a precisely larger dimension of 40×48×1.6mm3. The reconfigurable antenna performance can be enhanced by the number of active components of RF system employed [7], [8]. Reconfigurable antenna decreases the necessity of the various individual antennas working at different frequencies. In [9], high gain and pattern-reconfigurable patch antenna with different modes. RF modules are fabricated utilizing reconfigurable switched more-band antennas to serve various applications at remarkable frequency bands [10]. A Micromachined- switch based on reconfigurable surfaces is presented in the literature [11] Circularly-polarized reconfigurable patch antenna with liquid dielectric [12]. Manufacture of antennas integrated into RF-MEMS switches decreases the power loss and the parasitic impacts when contrasted with conventional solid-state switches. MEMS switches significantly focus on the decrease of size, weight, and cost of the component and additionally support high linearity over the various frequencies [13], [14]. A flexible

© 2024 The Authors. This work is licensed under a Creative Commons Attribution-NonCommercial-NoDerivatives 4.0 License.
For more information, see https://creativecommons.org/licenses/by-nc-nd/4.0/

material is used in [15] and operates at WiMAX applications presented with lower gain.

MEMS advancements offer a few preferences, for example, insignificant power loss and lower insertion loss over their traditional parts, such as PIN and RF CMOS switches [16], [17]. Correlating at the two frequencies is demanding and utilizing PIN diodes makes the tuning procedure difficult for current utilization [18], [19]. As well as power handling is reduced by embedding the semiconductor RF switches [20], [21]. Further, MEMS switches significantly focus on decreasing the size, weight, and cost components and additionally support high linearity over the various frequencies of different power levels. Few literatures are presented on microscale structures and reconfigurable antenna for 5G are reported in [22], [23]. Different authors [1], [2], [3], [4], [5], [6], [7], [8], [9], [10], [11], [12], [13], [14], [15], [16], [17], [18], [19], [20], [21], [22], [23], [24], [25], [26] perform the reconfigurability perspectives however restricted to a single operating frequency. The current work shows the advancement of a model double operating frequency reconfigurable antenna incorporation of a switch on a common substrate. The reconfigurable [27], [28] structure is presented with the transmitting edges. The pattern reconfigurability of different topology works [29] at two frequency bands all while which can be tuned by differing capacitance related to MEMS switches. The leaf-shaped patch antenna [30], triple elliptical [31], reconfigurable [32] antennas are presented for 5G applications.

This paper reports about a new kind of switch [37] used in antennas that can work across different frequencies. The switch is designed to be efficient, needing low voltage to work and being fast in switching with good isolation and low signal loss even at high frequencies. In [38] a new type of RF MEMS switch intended for antennas that can change frequencies depending upon how switch is positioned It uses special transmission lines to optimize its performance. In [39] a new type of antenna that can change its frequency range by using special switches. These switches adjust certain parts of the antenna, allowing it to work over a wider range of frequencies. Through a method called particle swarm optimization, the antenna's design was fine-tuned to operate effectively between 2 GHz and 3.2 GHz, with half of its bandwidth available at 2.4 GHz. In [40] This paper talks about a Ka-band patch antenna that can change its radiation pattern using RF MEMS switches. By controlling these switches, the antenna can have three different radiation patterns at 35 GHz. More research is needed to improve its signal coverage and reliability. In [41] a small L-slot antenna that can change its frequency using MEMS switches. It's designed for the U-band and measures 4.07 $\times$ 5.27 mm^2. The antenna has switches at the corner of the L-slot, allowing it to switch between four different frequencies from 42.36 GHz to 56.72 GHz for future communication systems.

The reconfigurable antennas with RF-MEMS switches for IoT, wireless, and 5G applications are limited. However,

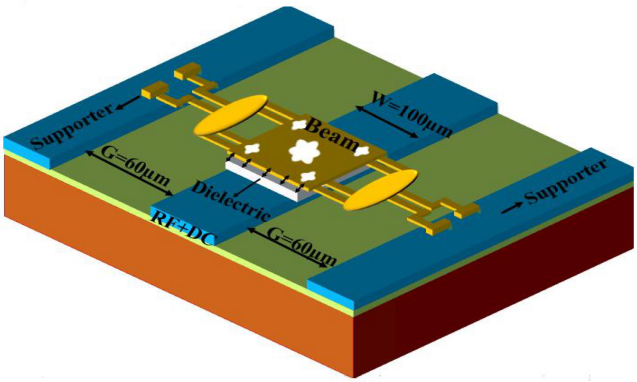

FIGURE 1. The proposed RF-MEMS Switch.

some antennas are presented, but the characteristics of the antennas like gain, bandwidth, reflection coefficient, and overall, parameters are also presented in this article. The main aim of this work, is to design a compact antenna with an RF-MEMS switch for reconfigurable at 5G applications. This paper is presented in 4 parts; part 2, gives the reconfigurable ESP antenna design and specifications and includes the MEMS switch structure details in the description. Part 3, convey results and discussion of the ESP antenna with four switching states of operations are presented. At last part 4 is dedicated to the conclusion of the model antenna.

II. ESP ANTENNA WITH RF-SWITCH DESIGN

In this work, a reconfigurable elliptical-shaped patch (ESP) antenna is presented, and it is incorporated with four MEMS switches and the proposed antenna model is resonates at dual bands with bandwidth of (7.76-8.6GHz) 840MHz and (10.26-10.79GHz)530MHz can be used for 5G applications. The proposed shunt capacitive switch is integrated to the ESP antenna operates at different switching modes (ON and OFF states)and the reconfigurability is achieved for frequency and the radiation pattern with dual resonant bands. The efficiency of the antenna is not affected by the incorporation of multiple switches to the patch.

A. RF-MEMS SWITCH DESIGN

The proposed ESP antenna design is realized by adding RF-MEMS shunt-capacitive-switch on to the ESP antenna. MEMS switch is realized with 50Ω transmission line. Switch dimensions are illustrated in the Fig. 1. Here, the RF-switch membrane is designed with the optimized dimensions of length and width are 350$\times$150μm^2 respectively. The geometry of the switch is illustrated in Table 1.

The switch actuates in different modes of operation (ON and OFF). The RF- switch is actuated with the actuation-voltage on to the beam. When the switch actuates it makes electrical contact with the lower electrode. The switch membrane is validated through electromechanical performance parameters such as actuating voltage, the time

TABLE 1. The parameters of the proposed novel MEMS switch.

Parameter	value	Parameter	value
Length	350 μm	Actuation voltage (V)	5.02
Width	150 μm	Switching Time(μs)	26 μs
Height	3μm	Switch resistance (mΩ)	0.4
Thickness	1μm	Isolation	-75dB at 10.1GHz
Holes	8×20 μm^2	Insertion loss	-0.07
Conduct area	100×150μm	Conduct Force (μN)	3e-6

taken from ON to OFF states of the switch and the lumped parameters like inductance, resistance and the capacitance. The dielectric thickness is considered for the proposed switch are $0.3\mu m$ and the beam thickness is of $1\mu m$ respectively. The simulated frequency response and the impedance matching is validated for the proposed switch. Mathematical Modeling of the proposed switch is given as follows. To calculate the RF parameters of the proposed switch, the lumped RLC components are to be considered to control the voltage from the signal line. The RLC components are presented in detail in the following equations. The operation mechanism depends on these parameters. Thus, the resistance and inductance and capacitance are given below with the following equations (1-3). Total inductance of the proposed switch can be calculated with the following equation. The parameters of the RF-switch can be obtained from equations (1-5).

$$L = 0.002l\left(\ln\frac{2l}{w+t} + 0.50049 + \frac{w+t}{3l}\right) \quad (1)$$

$$\text{The resistance is given as } R = \rho\frac{L}{S} \quad (2)$$

The capacitance at ON and OFF state is presents in below as

$$C_u \approx \varepsilon_0\frac{A}{g};\ C_d = \varepsilon_0\varepsilon_r\frac{A}{t_d} \quad (3)$$

The proposed RF-MEMS switch operating frequency is given as,

$$f = \frac{1}{2\pi}\sqrt{\frac{k}{m}} \quad (4)$$

The proposed RF-MEMS switch, switching time to be calculated by

$$t_s = 3.67\frac{V_p}{V_s}\sqrt{\frac{m}{k}} \quad (5)$$

where, m= Mass of the beam, k= Spring constant, V_p = pull-in voltage and V_s = switching voltage of the switch.

The fabrication of the proposed RF-MEMS switch with surface-micromachining flow is presents in Figure 2. Here four level masking process is used for the fabrication of the MEMS-switch presents in Figure 2(a-j). Here, firstly the wafer is cleaned with RCA process. and through oxide process Oxidation of test wafer is produced presents in Fig. 2(a). Similarly, the step-by-step fabrication of proposed RF-MEMS switch is done through surface micromachining process presented in Figure 2. Through sputtering and lithography process CPW metal layer is patterned. Dielectric layer is deposited using lithography. Using photo resists and lithography the sacrificial layer is deposited and patterned. The top layer is patterned using the steps of sputtering, photolithography. and critical point drying.

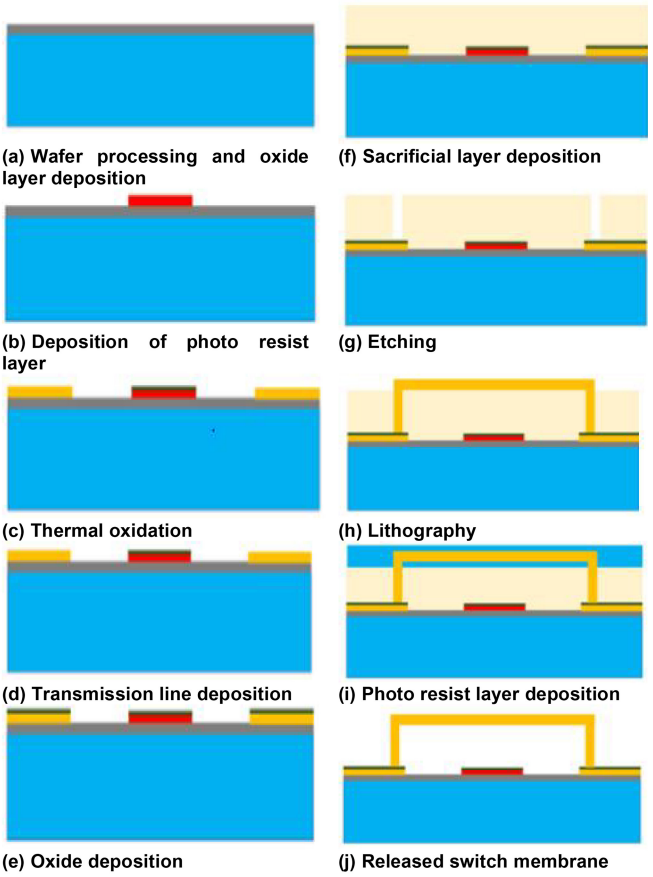

FIGURE 2. The fabrication flow of the proposed RF-MEMS switch with surface micromachining process.

The lumped equivalent circuit of the shunt capacitive switch is shown in Figure 3. The capacitance developed between the electrodes, resistance offered by beam and inductance due to ground plane and top electrode are in series to each other and parallel to the input. When no actuation voltage is applied the beam remains in upstate leading to low capacitive path for RF input. Therefore, the switch condition is said to be in ON state as shown in Figure 3a. Here, the signal cannot pass across RF MEMS switch the whole signal is transferred to the output terminal.

In the ON state, when the voltage is applied between the beam and lower electrodes, electrostatic forces cause

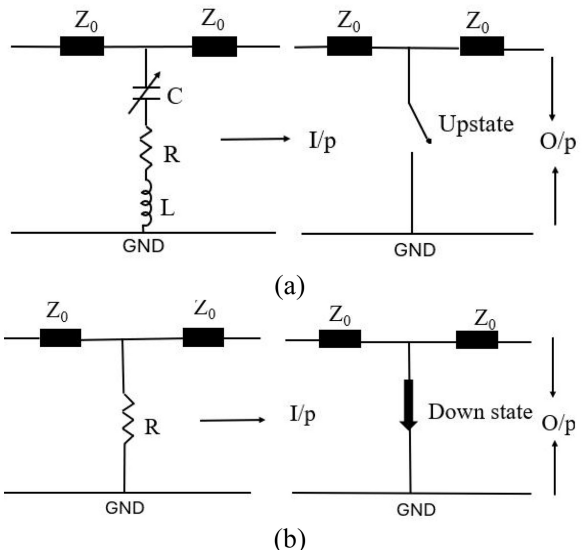

FIGURE 3. 3 Equivalent circuit model is desired for (a)ON state and (b)OFF state of the switch.

the beam to move downward, increasing the capacitance between them. This change in capacitance affects the overall impedance of the RF MEMS switch, as described by a specific equation (6)

$$Z_0 = R + j\omega L + \frac{1}{j\omega C} \tag{6}$$

The total impedance of the switch, denoted by Z_0, comprises the resistance (R), inductance (L), and capacitance (C) developed by the switch.

During the downstate of the beam, the switch provides a resistive path for signal transmission, facilitating the OFF condition, as depicted in Figure 3(b) When the impedance offered by the capacitance and inductance equals each other at the downstate, the impedance offered by the switch becomes resistive. This relationship is described by equations (7) and (8).

$$XL = XC \tag{7}$$

$$j\omega L = \frac{-1}{j\omega C} \tag{8}$$

The device's RF performance is assessed using lumped elements, The typical values of these components is crucial, particularly the capacitance values in both the switch's on and off states are important as indicated in the equivalent circuit.

B. ESP ANTENNA DESIGN

The reconfigurable elliptical-shaped patch (ESP) antenna is shown in Figure 4. The ESP antenna is designed on FR4 with the thickness of 1.59mm and $\varepsilon_r$is 4.4. The ESP antenna has dimensions of 28×30 mm^2 length and width of the patch. The half-moon elliptical shaped slots are etched on the patch and also elliptical shaped slot with rectangular strip line is also presented in the top

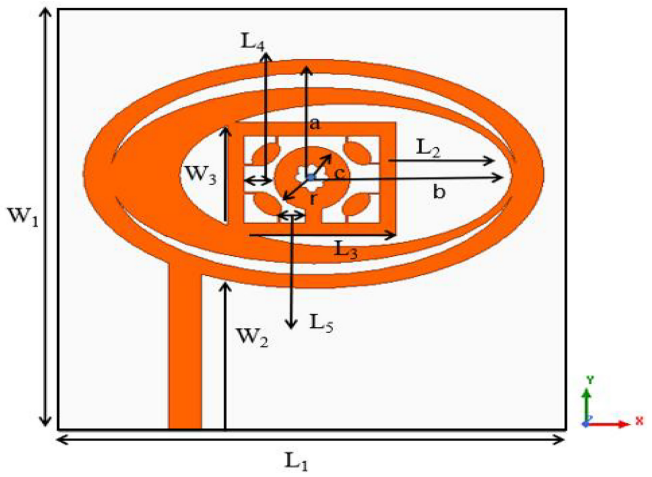

FIGURE 4. The front view of ESP antenna.

TABLE 2. Geometry of the ESP antenna.

Parameters	Values (mm)
L_1	28.0
W_1	30.0
W_2	12.0
W_3	8.0
L_2	9.0
a	13.6
b	12.4
c	2.25
L_3	10.0
L_4	1.2.0
L_5	0.8

side of the substrate, in the bottom side of the substrate is considered as full ground. In rectangular strip, slotted-circular patch and four strip lines are connected to the four corners of the rectangular strip lines. The proposed methodology is improving the directional characteristics of ESP antenna. The small values of eccentricity are realized to produce less reflection coefficient and good directional characteristics.

The ESP antenna optimized dimensions are given below in Table 2. The fundamental frequency is calculated by the resonance frequency equation of elliptical patch presented from Equations (9-14).The performance parameters of the ESP antenna are given in Table 3.

$$f_1 = \frac{1.8412V_0}{2a_{eff}\pi\sqrt{\varepsilon_r}} \tag{9}$$

$$a_{eff} = a\left[1 + \frac{2h}{\pi\varepsilon_r a}\left\{\ln\left(\frac{a}{2h}\right) + (1.41\varepsilon_r + 1.77)\frac{h}{a}(0.268\varepsilon_r + 1.65)\right\}\right]^{1/2} \tag{10}$$

$$f_{11}^{e,0} = \frac{15}{\pi e a_{eff}}\sqrt{\frac{q_{11}^{e,0}}{\varepsilon_r}} \tag{11}$$

$$q_{11}^{e} = -0.0049e + 3.7888e^2 - 0.7278e^3 + 2.314e^4 \tag{12}$$

TABLE 3. Performance parameters of the ESP antenna.

Parameter	Simulated	Measured
Resonant frequency (GHz)	8.34, 10.47	8.36,10.5
Reflection coefficient(dB)	-32.28, -22.73	-23.88, -29.29
Gain (dBi)	2.8	2.9
Radiation Efficiency (%)	86	77
Bandwidth (MHz)	840, 530	800, 510

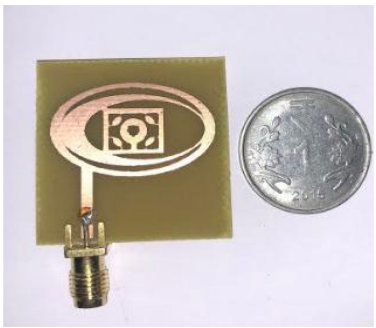

FIGURE 5. The fabricated ESP antenna model.

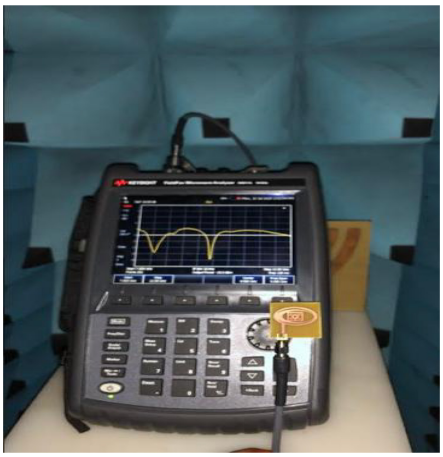

FIGURE 6. The measurement of the ESP antenna with VNA.

$$q_{11}^{\circ} = -0.0063e + 3.8316e^2 - 1.135e^3 + 5.2229e^4 \quad (13)$$

$$e = \frac{c}{a} \quad (14)$$

where ε_r=Permittivity, υ_0= speed of the light, a_{eff} =effective-radius, a= semi-major axis, $f_{11}^{e,0}$ = Dual-resonant frequency and q_{11}^{e} = Mathieu-function of dominant-mode, e= ellipse Eccentricity.

In this article the reflection coefficient, directional characteristics and gain of the ESP antenna are simulated and verified through measurements. The ESP antenna prototype is presented in Figure 5. The ESP antenna is fabricated and tested in anechoic chamber with VNA.is given in Figure 6. Figure 7 presents simulated and measured values of reflection coefficient of ESP antenna, here, simulated results are matched well with the measured results. However, a slight

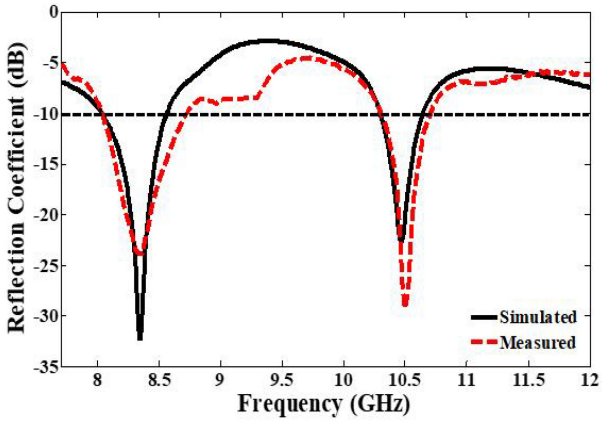

FIGURE 7. The S11 of the ESP antenna.

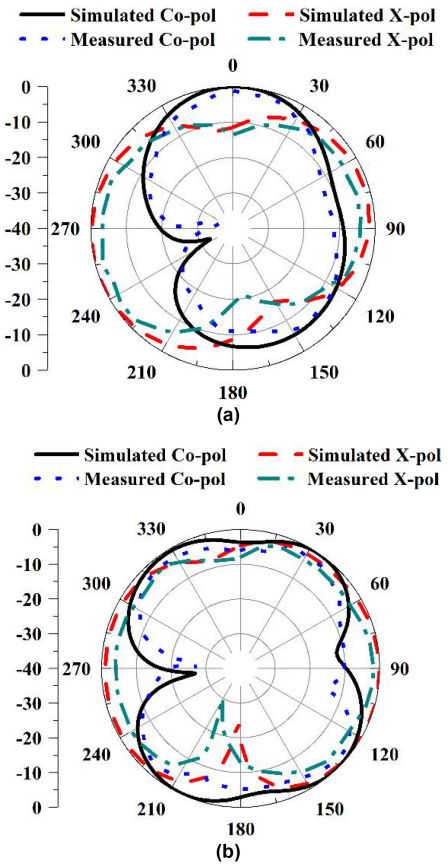

FIGURE 8. The simulated and measured Co-pol and X-polar of the ESP antenna at (a) 8.34 GHz, and (b) 10.47 GHz.

variation was found due to fabrication errors and parasitic effects.

The simulated and measured co-polarization (Co-polar) and cross-polarization (X-pol) are reported in Figure 8 at dual bands of the ESP antenna.

C. RECONFIGURABLE ESP ANTENNA WITH RF-SWITCH

The ESP antenna is incorporated with MEMS switch is presents in Figure 9. Here, specifications of ESP antenna and

TABLE 4. Different switching states of ESP antenna with four MEMS RF-switches.

Operation States	$S_{1.}$	$S_{2.}$	$S_{3.}$	$S_{4.}$	Resonant frequency (GHz)	Reflection coefficient (dB)	Gain (dBi)
State1	OFF	OFF	OFF	OFF	8.4,10.52	-20.0, -16.8	2.28,2.18
State2	OFF	OFF	OFF	ON	8.48,10.5	-20.49, -16.7	2.15, 2.1
State3	OFF	OFF	ON	OFF	8.47,10.49	-21.7, -17.4	2.12,2.03
State4	OFF	OFF	ON	ON	8.46,10.55	-22.0, -17.04	2.08,1.30
State5	OFF	ON	OFF	OFF	8.49,10.44	-19.6, -15.9	2.54,2.99
State6	OFF	ON	OFF	ON	8.43,10.47	-22.3, -17.3	2.08,2.13
State7	OFF	ON	ON	OFF	8.49,10.5	-20.6, -15.9	2.11,2.62
State8	OFF	ON	ON	ON	8.5,10.44	-19.9, -19.3	2.59,2.57
State9	ON	OFF	OFF	OFF	8.49,10.45	-19.4-19.01	2.26,2.06
State10	ON	OFF	OFF	ON	8.48,10.43	-19.8, -17.7	2.24,2.32
State11	ON	OFF	ON	OFF	8.47,10.49	-21.3,-19.27	2.19,2.14
State12	ON	OFF	ON	ON	8.51,10.45	-20.10, -19.5	2.34,2.85
State13	ON	ON	OFF	OFF	8.49,10.47	-19.2,-21.28	2.48,3.04
State14	ON	ON	OFF	ON	8.5,10.46	-20.8,-18.5	2.47,3.90
State15	ON	ON	ON	OFF	8.52,10.46	-20.3,-17.8	2.2,2.87
State16	ON	ON	ON	ON	8.49,10.49	-21.3,-31.6	2.58,2.64

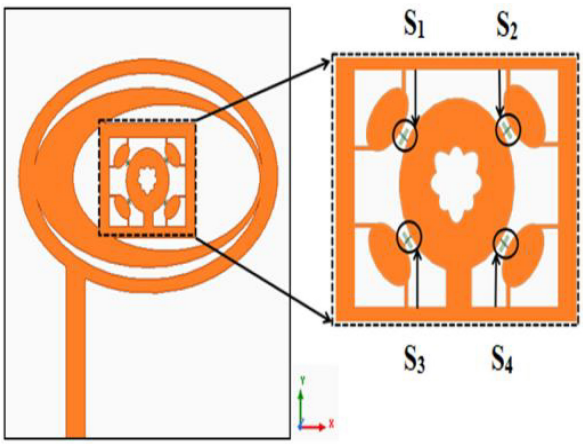

FIGURE 9. The reconfigurable ESP antenna with close view of MEMS switches.

RF-switch are discussed in the above sections. The reflection coefficient at all the switching states is discussed in the Table 4. The reconfigurable ESP antenna is used for 5G applications.

The ON / OFF conditions of RF-switch make the antenna resonate with dual bands at X band frequency, the switching reconfiguration of frequency and radiation patterns are achieved. The ESP antenna is controlled by RF-switches on the patch. In this work four switches are incorporated on rectangular strip line of the patch antenna to enhance the performance. During ON state the switch actuates towards the electrode, and it contacts the bottom dielectric. Frequency shift is observed with a bandwidth 400MHz at the X-band because of the capacitance variation of the proposed switch. Depending on the capacitance variation, the proposed switch the ESP antenna current distributions will be varied.

The process of analyzing the RF MEMS switch and reconfigurable antenna begins with optimization of the parameters using mathematical formulas. Thereafter, electromagnetic tools are employed to conduct simulation analyses, allowing for the assessment of the individual and combined behavior of both components. Following the simulation analysis, the antenna undergoes a comprehensive performance evaluation to validate its functionality. Parameters such as resonant frequency, radiation pattern, and efficiency are thoroughly analyzed to ensure optimal performance. Similarly, a detailed assessment of the RF MEMS switch is carried out to verify its functionality, performance characteristics, switching time and reliability. The next step involves integrating the optimized designs and fabricating the proposed device. This integration process ensures good compatibility and operation between the antenna and switch. Fabrication describes physically constructing the antenna system according to the finalized design specifications. Once the device is fabricated, different measurements are conducted to validate the proposed models and confirm that the measured performance matches with the simulated results. This validation step ensures that the fabricated device meets the desired specifications or not. The step-by-step approach of the proposed ESP antenna with RF MEMS switch is given in the Figure 10.

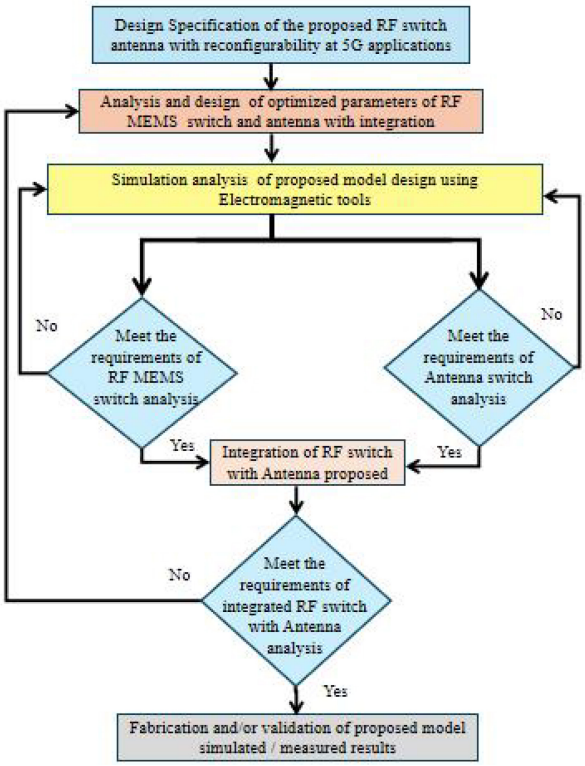

FIGURE 10. Step by step optimization model for the proposed switch with antenna.

III. RESULTS OF THE ESP ANTENNA

The analysis of proposed ESP antenna with RF-MEMS switch is analyzed. The characteristics of the proposed antenna are explained one by one in each subsection. S_{11} characteristics of proposed ESP antenna is explained in subsection A. Radiation pattern and surface current distribution of proposed ESP antenna is explained subsection B and C respectively.

A. S_{11} OF ESP ANTENNA

In this article, the implementation of reconfigurable ESP antenna and RF-MEMS switch is work at 5G communication applications. The antenna and the switch are realized by 50Ω impedance transmission line. The reflection coefficient (S11) of the all the states of proposed ESP antenna is analyzed. If the switch is realized with 50Ω then it is perfectly integrated on to the elliptical split patch. The ESP antenna and RF switching configuration can resonate the operating frequency is observed from 8.4-10.6 GHz to be lead the reconfigurability. By observing the switching modes, open or closed they may vary the dimension of the ESP antenna and the resonating frequency. The novel ESP antenna embedded with four MEMS switches connecting them together acts as a single patch. The ESP antenna reflection coefficient is observed in Figure 11 at four switching states with closer view. The frequency reconfigurability is observed for every switching state (state-1 to state-16). At state-1, state-4, state-13 and state-16 device performance is good. The rest of the states are presented in Table 4.

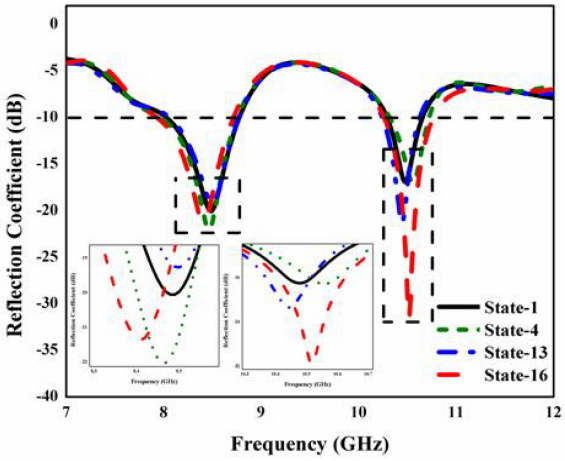

FIGURE 11. The reflection coefficient of (S_{11}) reconfigurable ESP antenna.

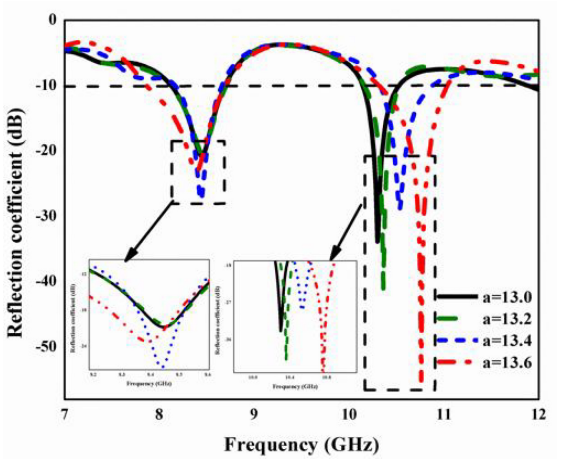

FIGURE 12. The S_{11} by varying semi major axis.

The ESP antenna is varying the semi-major and minor axis to optimize the ESP antenna for optimization. The reflection coefficient, directional patterns, current distributions, and gain are performed at four operating states of ESP antenna. The resonant frequency bands attained for all the switch configurations from 8.4GHz and 10.6 GHz. The resonant bands may shift towards the lower end or higher end depending on the lumped parameters and the switch configurations. Based on switching modes the length of the elliptical patch may vary from longer length to shorter length. The parametric analysis is observed at semi major and semi minor axis is also presented in Figure 12 and Figure 13 respectively of the proposed ESP antenna. However, the optimized parameters has good results.

B. RADIATION PATTERNS OF THE ESP ANTENNA

The radiation patterns of ESP antenna Co-pol and X-pol at dual frequency bands of four switching modes

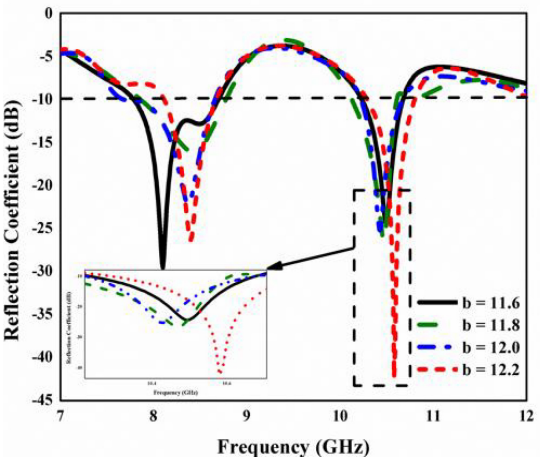

FIGURE 13. The S_{11} by varying semi minor axis.

are observed in Figure 14. Co-polarization means the antennas are transmitting and receiving signals in the same direction, which is beneficial for stronger signals. When the RF MEMS switch is ON, the antennas are aligned properly, enhancing the signal and reducing losses.

Cross-polarization occurs when antennas are misaligned, leading to signal issues. In the OFF state of the switch, misalignment can occur more frequently, impacting antenna performance. The Co-pol and X-pol for all the switching states in Figure 14 (a - d). From the results it is observed that the ESP antenna is able to change its patterns at one of the resonant bands of four switching states. The Co-pol and X-pol at four switching states are observed at 8.4GHz and 8.5GHz; 10.5GHz and 10.6GHz respectively. The patterns at four switching states operate at lower resonant band are almost similar. The ESP antenna works in different switching modes of operation. From the obtained results the proposed ESP antenna can realize the reconfigurability of radiation characteristics by actuating the different states of RF-switches. The ESP antenna can obtain reconfigurable property by altering the current phase elements. It is observed that the RF-switch is in ON-state, the current intensity on the radiating patch leads to increase there by radiation intensity increases. Similarly, in the OFF state of the switch the current intensity does not change. The ESP antenna resonates at two resonant bands. The ESP antenna simulated and measured, presents in Table 3. Different switching states of the ESP antenna with four MEMS switches are given in Table 4.

C. EFFICIENCY PLOTS OF THE ESP ANTENNA

The inclusion of an RF MEMS switch in the antenna design allows for changing the states of the switch, enhancing efficiency by frequency tuning and radiation pattern. In contrast, antennas without RF MEMS switches may lack such adaptability, leading to fixed characteristics and leading to reduced performance in varying conditions. Therefore,

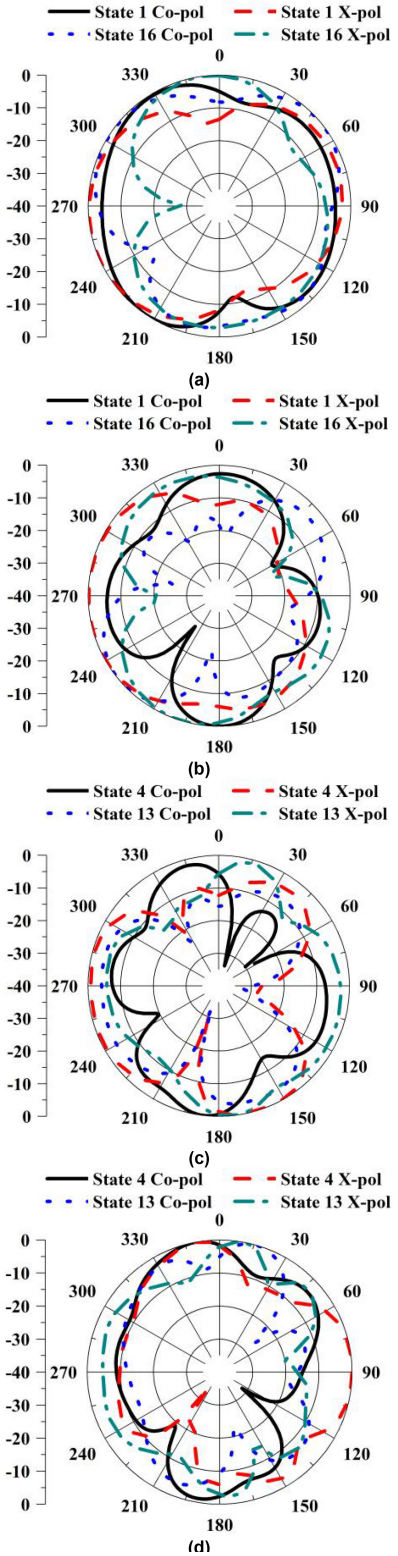

FIGURE 14. Radiation patterns of the proposed ESP antenna at different configurations with four switches state 1 and 16 at two resonant bands (a)8.4GHz (b)10.52GHz and at (b) state 4 and 13 state at (c) 8.46GHz (d) 10.55GHz.

integrating an RF MEMS switch significantly improves the antenna's efficiency for modern wireless communication systems. The efficiency plot with (86%) and without (77%)

TABLE 5. Comparison of the reconfigurable ESP antenna with previous works.

Ref No	Type of antenna	Material	Dimension of switch	Actuation Voltage (V)	Dimension of antenna (cm^3)	Resonant Frequency (GHz)	Reflection coefficient (dB)	Band Width (MHz)	Gain (dBi)	Application
7	U-shaped slot patch	Fr4	5×4×145 mm^3	3.3	50×32×1	4.9 3.5	<-10	200 900	3.6 3.8	5G Applications
10	ORIOL antenna	Quartz substrate	980×980 μm^2	30	50.8×50.8×1.575	3.82	<-10	500	4.9	5G Applications
18	Microstrip antenna	Roger	2.5×1.25 ×0.9mm3	0.82	30.3×24.8×0.8	UWB	<-15	123	-6	UWB
20	U-slotted antenna	FR-4	1.8×2mm^2	6	40×36×1.6	1.8/4.18/5.56	<-17.5, <-<-60	128	-5	Mobile, WLAN
21	Sierpinski antenna	LCP	400×200 μm^2	39.21	20×25×1.5	2.4-18	<-32	80	N/A	C,S and X band
39	Rectangular antenna	FR-4	225×100 μm^2	5.7	18×13×4	4.5-12	<-50	N/A	3.17	UWB
40	Rectangular patch	Rogers	320X80 μm^2	14	10×10×0.5	40	<-55	N/A	4.52	5G Applications
41	E shaped patch	Rogers RT5880	100X120 μm^2	0-90	10×12×0.157	2.0–2.6	<40	500	N/A	Cognitive Radio
42	Rectangular antenna	Silicon	320*110 μm^2	4.5	3.7×5.2×0.4	35	<-20	500	4	Smart phon application
43	L slot	Rogers RT5880	1000*1000 μm^2	8.59	5.27×4.07×0.25	42.6-53.08	<-25	>1 GHz	7	U band
This work	Elliptical Patch	FR4	100×160μm^2	5.02	28×30×1.6	8.34, 10.47	-32.28, -22.73	840, 530	3.04, 2.98	5G Applications

N/A: Not available

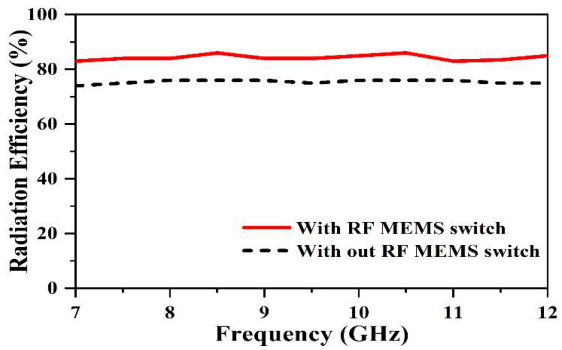

FIGURE 15. Comparison of the radiation efficiency of the proposed antenna with and without RF MEMS switch.

RF MEMS switches at two resonant bands are is given in Figure 15.

D. CONTOUR PLOTS OF THE ESP ANTENNA

The contour plots of the ESP antenna at corresponding resonant bands under each operating mode (state I, state II, state III, state IV). The resonating frequencies at state-1(state I) are 8.4GHz and 10.52GHz; state-4 (state II) are 8.56GHz and 10.55GHz; state-13 (state III) are 8.49GHz and 10.47GHz, and state-16 (state IV) are 8.49GHz and 10.49GHz are presented in Figure 16. Contour plots of the proposed design visually represent how these currents distribute when the RF MEMS switch is in its activated (ON) state, varying the antenna's performance characteristics. The contour plots differentiate between the ON and OFF states of the switch, demonstrating different patterns in current flow under each condition (state1, state4, state13, state16). By analyzing these contour plots, it is visible that how the RF MEMS switch integration optimizing antenna performance for different operating conditions and communication requirements. In the ON state, the contour plots may show concentrated current flow around specific regions of the patch, indicating enhanced radiation in certain directions. In the OFF state, the contour plots may exhibit more uniform current distribution across the patch, leading to different radiation pattern characteristics. The contour plots of the proposed design with RF MEMS switch for all the switching states are shown in Figure 16.

The RF-MEMS switch performance is observed better at four different conditions at state I has OFF-OFF-OFF-OFF conditions, state II has OFF-OFF-ON-ON conditions, state III has ON-ON-OFF-OFF conditions, and state IV has ON-ON-ON-ON are considered for validation. For each and every resonant band the surface-currents have along the surface of the ESP antenna. It is clearly observed that the effective length of ESP antenna is inversely proportional to the resonant frequencies. Here, current distributions are shown at four operating modes are presented in Figure 16. The radiating patch attains the linear polarization in four operating modes of the switch. While the switches are in ON state the current density is more.

E. 3D GAIN PLOTS OF THE ESP ANTENNA

Gain values vary across different switching states, indicating how the antenna's performance changes based on which MEMS RF-switches are activated or deactivated. The 3D gain plots of the ESP antenna at different switching states

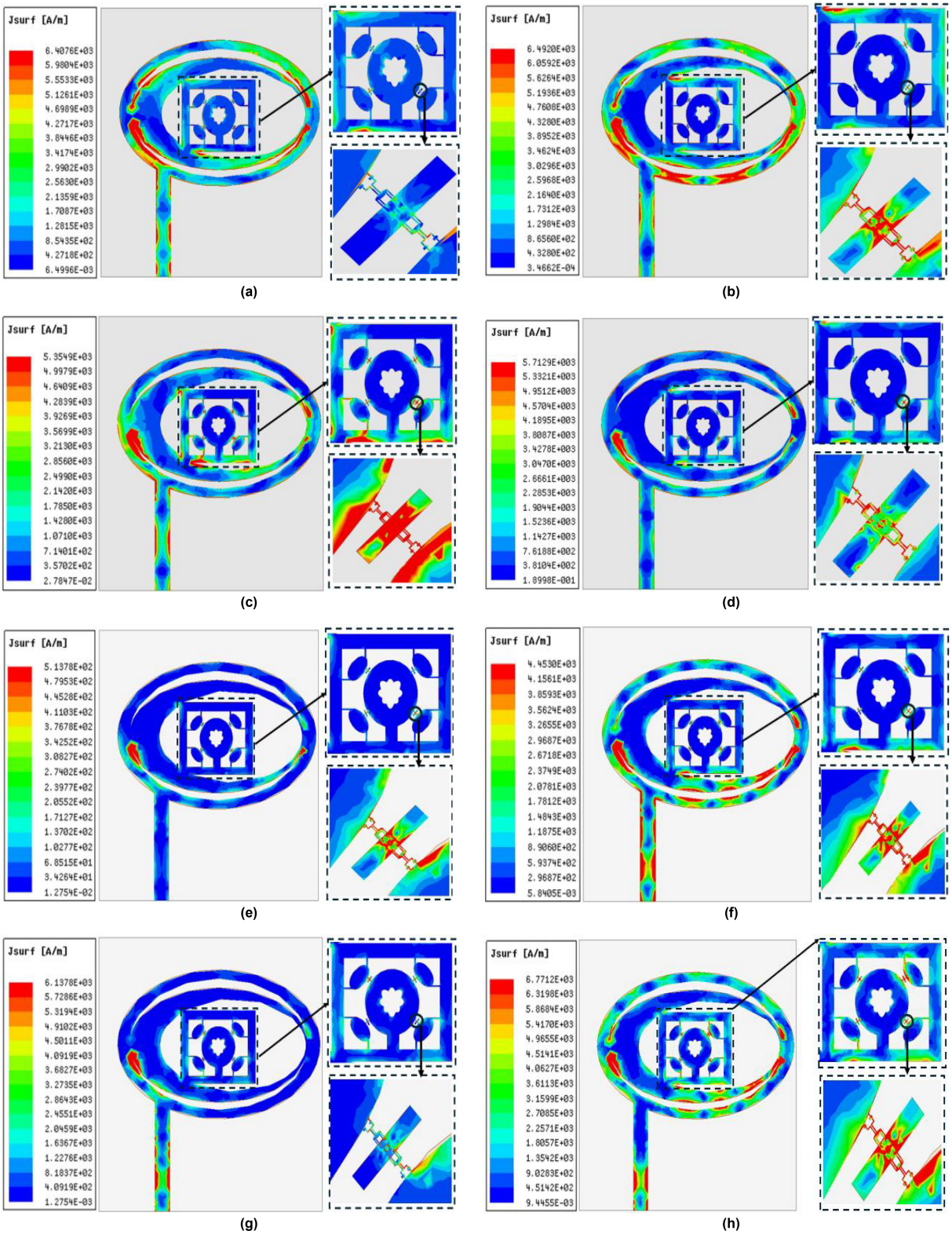

FIGURE 16. Contour plots of the reconfigurable ESP antenna at different switching states with four switchesstate-1 at two resonant bands (a) 8.4GHz and (b)10.52GHz, state-4at two resonant bands(c) 8.46GHz and (d) 10.55GHz, state-13 at two resonant bands (e) 8.5GHz and (f) 10.46GHz and state-16 at two resonant bands (g) 8.49GHz and (h)10.49 GHz.

with four switches is reported in Figure 17. The reconfigurable ESP antenna is presented with good performance with the presented works. 3D-gain plots of ESP antenna are observed in Fig. 17. The operating frequency and gains are observed at RF-MEMS switch is placed on patch for dual bands for four states. At the state-I, two operating frequencies

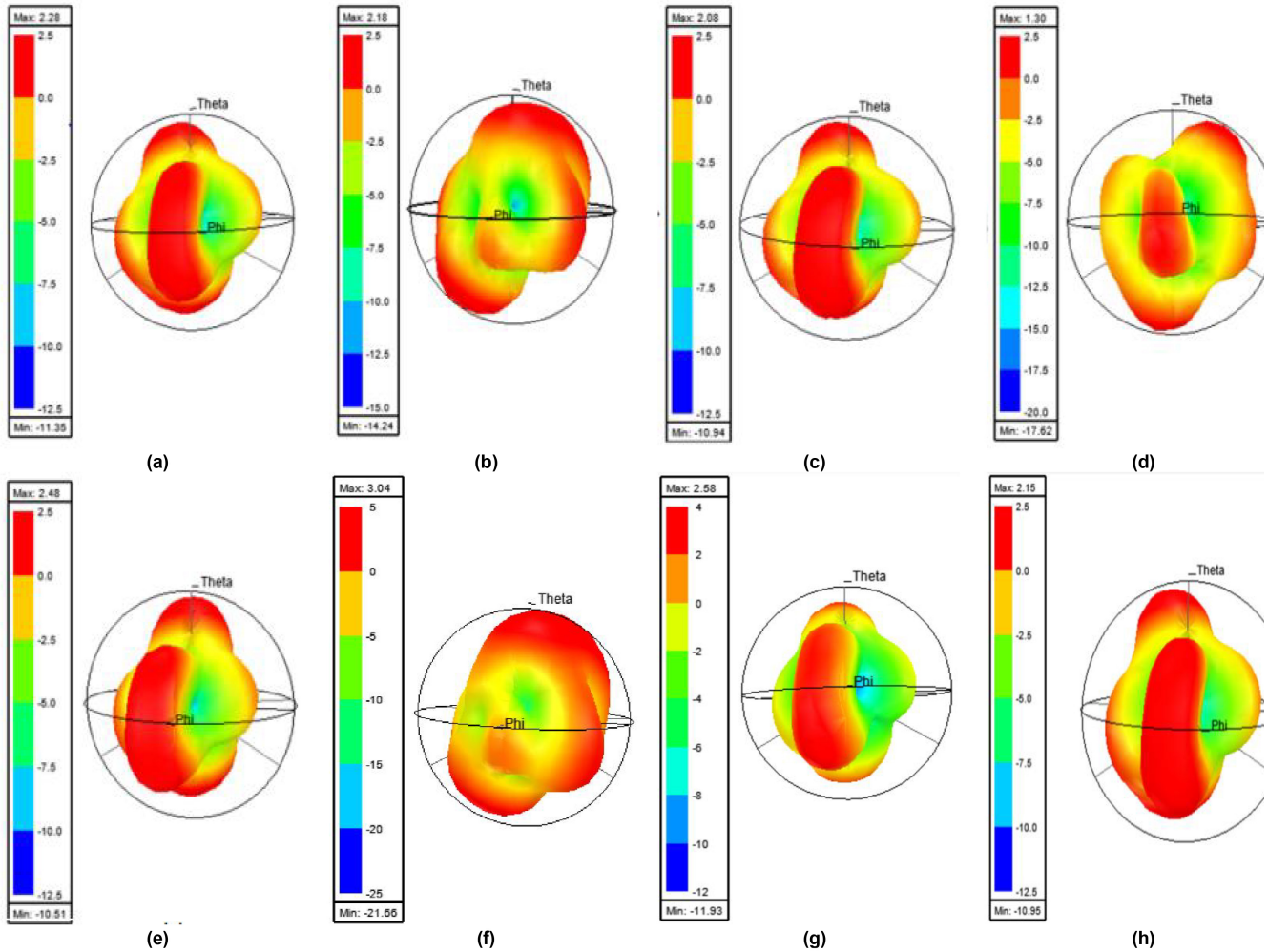

FIGURE 17. 3D gain plots of the reconfigurable ESP antenna at different switching states with four switches state-1 at two resonant bands (a) 8.4GHz and (b)10.52GHz, state-4at two resonant bands(c) 8.46GHz and (d) 10.55GHz, state-13 at two resonant bands (e)8.5GHz and (f) 10.46GHz and state-16 at two resonant bands (g) 8.49GHz and (h) 10.49 GHz.

and gain are 8.4GHz, 10.52GHz with 2.28dBi, 2.18dBi. Similarly, for state-II frequencies are 8.56GHz, 10.55GHz with gain of 2.08dBi, 1.30dBi; at state-III frequencies are 8.49GHz, 10.47GHz with gain of 2.48dBi and 3.04dBi; and state-IV, frequencies are 8.49GHz, 10.49GHz with gain of 2.58dBi, and 2.64dBi. The comparison table with existing work to previous work is presented in the Table 5.

IV. CONCLUSION

This work presents a reconfigurable elliptical shaped patch antenna with RF MEMS switches. The proposed antenna is obtained reconfigurability by loading the MEMS switches on to the patch surface, the reconfigurable elliptical-shaped patch antenna is resonating at 8.34GHz and 10.47GHz with reflection coefficient of −32.28dB and −22.7dB respectively. The reconfigurable ESP antenna operates at the frequency of 8.36GHz and 10.5GHz with reflection coefficient (S_{11}) of −23.88 dB and −29.29dB respectively. The operating frequencies and gains are observed at RF-MEMS switch is placed on patch for dual bands for four states. At the state-I, two operating frequencies and gain are 8.4GHz, 10.52GHz with 2.28dBi, 2.18dBi. Similarly, for state-II frequencies are 8.56GHz, 10.55GHz with gain of 2.08dBi, 1.30dBi; at state-III frequencies are 8.49GHz, 10.47GHz with gain of 2.48dBi and 3.04dBi; and state-IV, frequencies are 8.49GHz, 10.49GHz with gain of 2.58dBi, and 2.64dBi is observed. The radiating patch attains the linear polarization in four operating modes of the switch. The measurement analysis is performed using Keysight N9917A vector network analyzer (VNA) in the anechoic chamber. The simulated results are confirmed well with the measured results. The error estimation between the simulated and measured results are below ±5%. The obtained results show that ESP antenna can be used for 5G applications.

REFERENCES

[1] H. Huang, Y. Liu, S. Zhang, and S. Gong, "Multiband metamaterial-loaded monopole antenna for WLAN/WiMAX applications," *IEEE Antennas Wireless Propag. Lett.*, vol. 14, pp. 662–665, 2014.

[2] A. K. Gautam, L. Kumar, B. K. Kanaujia, and K. Rambabu, "Design of compact F-shaped slot triple-band antenna for WLAN/WiMAX applications," *IEEE Trans. Antennas Propag.*, vol. 64, no. 3, pp. 1101–1105, Mar. 2016.

[3] J. Navarajan, M. R. E. Jebarani, and V. G. Krishnan, "Design of frequency reconfigurable antenna based on μC-μEMS switch," *AEU Int. J. Electron. Commun.*, vol. 171, Nov. 2023, Art. no. 154911.

[4] S. A. Haydhah, F. Ferrero, L. Lizzi, M. S. Sharawi, and A. Zerguine, "A multifunctional compact pattern reconfigurable antenna with four radiation patterns for sub-GHz IoT applications," *IEEE Open J. Antennas Propag.*, vol. 2, pp. 613–622, 2021.

[5] M. M. Hassan, "Two element MIMO antenna with frequency reconfigurable characteristics utilizing RF MEMS for 5G applications," *J. Electromagn. Waves Appl.*, vol. 34, no. 9, pp. 1210–1224, 2020.

[6] C.-Y. Chiu, J. Li, S. Song, and R. D. Murch, "Frequency-reconfigurable pixel slot antenna," *IEEE Trans. Antennas Propag.*, vol. 60, no. 10, pp. 4921–4924, Oct. 2012.

[7] B Khalichi, S Nikmehr, and A Pourziad, "Reconfigurable SIW antenna based on RF-MEMS switches," *Progr. Electromagn. Res.*, vol. 142, pp. 189–205, Aug. 2013.

[8] A. Grau, J. Romeu, M.-J. Lee, S. Blanch, L. Jofre, and F. De Flaviis, "A dual-linearly-polarized MEMS-reconfigurable antenna for narrowband MIMO communication systems," *IEEE Trans. Antennas Propag.*, vol. 58, no. 1, pp. 4–17, Jan. 2010.

[9] K.-D. Hong, X. Zhang, L. Zhu, and T. Yuan, "A high-gain and pattern-reconfigurable patch antenna under operation of TM and TM modes," *IEEE Open J. Antennas Propag.*, vol. 2, pp. 646–653, 2021.

[10] K. K. Naik and P. A. V. Sri, "Design of hexadecagon circular patch antenna with DGS at Ku band for satellite communications," *Progr. Electromagn. Res.*, vol. 63, pp. 163–173, Jan. 2018.

[11] A. Karimi, U. Shah, S. Yu, and J. Oberhammer, "A high-performance 220-290 GHz micromachined-waveguide switch based on interference between MEMS reconfigurable surfaces," *IEEE Trans. Thz Sci.*, vol. 14, no. 2, pp. 188–198, Mar. 2024.

[12] Z. Chen, H.-Z. Li, H. Wong, X. Zhang, and T. Yuan, "A circularly-polarized-reconfigurable patch antenna with liquid dielectric," *IEEE Open J. Antennas Propag.*, vol. 2, pp. 396–401, 2021.

[13] P. Y. Chen and A. Alu, "Dual-mode miniaturized elliptical patch antenna with μ-negative metamaterials," *IEEE Antennas Wireless Propag. Lett.*, vol. 9, pp. 351–354, 2010.

[14] R. Alhamad, E. Almajali, and S. Mahmoud, "Electrical reconfigurability in modern 4G, 4G/5G and 5G antennas: A critical review of polarization and frequency reconfigurable designs," *IEEE Access*, vol. 11, pp. 29215–29233, 2023.

[15] G. Dattatreya and K. K. Naik, "A low volume flexible CPW-fed elliptical-ring with split-triangular patch dual-band antenna," *Int. J. RF Microw. Comput.-Aided Eng.*, vol. 29, no. 8, 2019, Art. no. e21766.

[16] K. R. Shashikant and A. Kulkarni, "Reconfigurable patch antenna design using pin diodes and raspberry PI for portable device application," *Wireless Pers. Commun.*, vol. 112, no. 3, pp. 1809–1828, 2020.

[17] Y. Jang, J. Choi, and S. Lim, "Frequency reconfigurable zeroth-order resonant antenna using RF MEMS switch," *Microw. Opt. Technol. Lett.*, vol. 54, no. 5, pp. 1266–1269, May 2012.

[18] M. Bemani and S. Nikmehr, "A novel reconfigurable multiband slot antenna fed by a coplanar waveguide using radio frequency microelectro-mechanical system switches," *Microw. Opt. Technol. Lett.*, vol. 53, no. 4, pp. 751–757, Apr. 2011.

[19] K. K. Naik and D. Gopi, "Flexible CPW-fed split-triangular shaped patch antenna for WiMAX applications," *Progr. Electromagn. Res.*, vol. 70, pp. 157–166, Jul. 2018.

[20] H. Oraizi and N. V. Shahmirzadi, "Frequency-and time-domain analysis of a novel UWB reconfigurable microstrip slot antenna with switchable notched bands," *IET Microw. Antennas Propag*, vol. 11, no. 8, pp. 1127–1132, Feb. 2017.

[21] D. Sanchez-Escuderos, M. Ferrando-Bataller, M. Baquero-Escudero, and J. I. Herranz, "Reconfigurable slot-array antenna with RF-MEMS," *IEEE Antennas Wireless Propag. Lett.*, vol. 10, pp. 721–725, 2011.

[22] K. Ramahatla, M. Mosalaosi, A. Yahya, and B. Basutli, "Multiband reconfigurable antennas for 5G wireless and CubeSat applications: A review," *IEEE Access*, vol. 10, pp. 40910–40931, 2022.

[23] N. Kingsley, D. E. Anagnostou, M. Tentzeris, and J. Papapolymerou, "RF MEMS sequentially reconfigurable sierpinski antenna on a flexible organic substrate with novel DC-biasing technique," *J. Microelectromech. Syst.*, vol. 16, no. 5, pp. 1185–1192, Oct. 2007.

[24] T. Ali, M. M. Khaleeq, and R. C. Biradar, "A multiband reconfigurable slot antenna for wireless applications," *Int. J. Electron. Commun.*, vol. 84, pp. 273–280, Feb. 2018.

[25] M. Donelli and J. Iannacci, "Exploitation of RF-MEMS switches for the design of broadband modulated scattering technique wireless sensors," *IEEE Antennas Wireless Propag. Lett.*, vol. 18, pp. 44–48, 2019.

[26] E. A. Savin, K. A. Chadin, and R. V. Kirtaev, "Design and manufacturing of X-band RF MEMS switches," *Microsyst. Technol.*, vol. 24, no. 6, pp. 2783–2788, 2018.

[27] K. Demirel, E. Yazgan, S. Demir, and T. Akin, "A new temperature-tolerant RF MEMS switch structure design and fabrication for Ka-Band applications," *J Microelectromech. Syst.*, vol. 25, no. 1, pp. 60–68, Feb. 2016.

[28] E. Brusa, G. De Pasquale, and A. Somà, "Experimental characterization of electro–thermo–mechanical coupling in gold RF microswitches," *J. Microelectromech. Syst.*, vol. 22, no. 4, pp. 919–929, Aug. 2013.

[29] L.-Y. Ma, N. Soin, M. H. M. Daut, and S. F. W. M. Hatta, "Comprehensive study on RF-MEMS switches used for 5G scenario," *IEEE Access*, vol. 7, pp. 107506–107522, 2019.

[30] I. E. Lysenko, A. V. Tkachenko, O. A. Ezhova, B. G . Konoplev, E. A. Ryndin, and E. V. Sherova, "The mechanical effects influencing on the design of RF MEMS switches," *Electronics*, vol. 9, no. 2, p. 207, 2020.

[31] S. Tang, Y. Zhang, Z. Han, C.-Y. Chiu, and R. Murch, "A pattern-reconfigurable antenna for single-RF 5G millimeter-wave communications," *IEEE Antennas Wireless Propag. Lett.*, vol. 20, no. 12, pp. 2344–2348, Dec. 2021.

[32] C. X. Mao, L. Zhang, M. Khalily, and P. Xiao, "Single-pole double-throw filtering switch and its application in pattern reconfigurable antenna," *IEEE Trans. Antennas Propag.*, vol. 70, no. 2, pp. 1581–1586, Feb. 2022.

[33] S. Zhao, Z. Wang, and Y. Dong, "A planar pattern-reconfigurable antenna with stable radiation performance," *IEEE Antennas Wireless Propag. Lett.*, vol. 21, pp. 784–788, 2022.

[34] N. Supreeyatitikul, P. Janpangngern, T. Lertwiriyaprapa, M. Krairiksh, and C. Phongcharoenpanich, "CMA-based quadruple-cluster leaf-shaped metasurface-based wideband circularly-polarized stacked-patch antenna array for sub-6 GHz 5G applications," *IEEE Access*, vol. 11, pp. 14511–14523, 2023.

[35] M. Ayyappan and P. Patel, "On design of a triple elliptical super wideband antenna for 5G applications," *IEEE Access*, vol. 10, pp. 76031–76043, 2022.

[36] B. Rana, S.-S. Cho, and I.-P. Hong, "Review paper on hardware of reconfigurable intelligent surfaces," *IEEE Access*, vol. 11, pp. 29614–29634, 2023.

[37] S. Goel and N. Gupta, "Design, optimization and analysis of reconfigurable antenna using RF MEMS switch," *Microsyst. Technol.*, vol. 26, no. 9, pp. 2829–2837, 2020.

[38] Y. Xu, Y. Tian, B. Zhang, J. Duan, and L. Yan, "A novel RF MEMS switch on frequency reconfigurable antenna application," *Microsyst. Technol.*, vol. 24, pp. 3833–3841, Sep. 2018.

[39] H. Rajagopalan, J. M. Kovitz, and Y. Rahmat-Samii, "MEMS reconfigurable optimized E-shaped patch antenna design for cognitive radio," *IEEE Trans. Antennas Propag.*, vol. 62, no. 3, pp. 1056–1064, Mar. 2014.

[40] Z. Deng, Y. Wang, and C. Lai, "Design and analysis of pattern reconfigurable antenna based on RF MEMS switches," *Electronics*, vol. 12, no. 14 p. 3109, 2023.

[41] Y. Chen et al., "An L-slot frequency reconfigurable antenna based on MEMS technology," *Micromachines*, vol. 14, no. 10, p. 1945, 2023.

KETAVATH KUMAR NAIK (Senior Member, IEEE) received the B.Tech. degree in electronics and communication engineering from the Jawaharlal Nehru Technological University (JNTU), JNTU College of Engineering, Hyderabad, India, the M.Tech. degree from the JNTU College of Engineering, Anantapur, India, and the Ph.D. degree in electronics and communication engineering from the College of Engineering, Andhra University, Visakhapatnam, India.

He is working as a Professor with the Department of Electronics and Communication Engineering, Koneru Lakshamaiah Educational Foundation (Deemed to be University), Guntur, India. He is also authored 5 book chapters and has 7 patents. He was listed in Top 2% influenced Scientists Worldwide, Elsevier (Scopus), by Stanford's University, USA in 2021, 2022, and 2023. He has sponsored research projects from the Department of Science and Technology (DST) and Council of Scientific and Industrial Research. He also received the "DST Young Scientist Award" in 2014 from the Government of India, "Best Researcher Award" from KLEF University in 2021, 2022, and 2023, Best Teacher Award in 2021 from SFLT, Regd. by Government of AP, and a Distinguished Research Award in 2021 from IJIEMR – Elsevier SSRN. He is the Referee for Sponsored Research Proposals of DST, SERB, CSIR, and Government of India. He is Referee of Sponsored Research Proposal of Science and Engineering Research Board, DST, Government of India. He is an Associate Editor of *International Journal of Electronics, Communications, and Measurement Engineering*, IGI Global, USA. He is a Reviewer for various international and national journals and conferences. He is a Fellow of *Institution of Electronics and Telecommunication Engineers*.

BOKKISAM VENKATA SAI SAILAJA was born in Andhra Pradesh, India. She received the B.Tech. degree from Anna university, Chennai, India, in 2012, and the Ph.D. degree in electronics and communication engineering from the Koneru Lakshmaiah Education Foundation (KLEF) Guntur. She worked as CSIR-SRF from April 2021 to March 2023. Her achievements also include project execution through Indian Nanoelectronics Users Program. Since 2023, she is currently working as an Assistant professor with the Department of Electronics and Communication Engineering, KLEF. She has published 21 papers in international, national journals, and conferences. Her research interests include reconfigurable antenna's, and RF MEMS switches for wireless communications.